The Tibetan plateau is for the most part underlain by rocks of pre-Cenozoic age, a fact that has hindered the identification of Cenozoic shortening structures that can be unequivocally related to the effects of India-Asia collision. Notably, however, the Qiangtang block contains a number of small, short wavelength basins filled with terrestrial sediments of early Tertiary age. Where these basins have been well studied, sedimentation is recognized as having occurred coevally with compressional deformation. The classic treatment of compressional basins appeals to accommodation space created by the flexure of an elastic plate in response to loads created by adjacent thrust fault bound ranges. It is unlikely that the Tertiary basins of the Qiangtang block formed in this manner. The wavelength of a classically modelled flexural basin is a basically a function of the thickness of the elastic plate and the density difference between sedimentary fill and ductile material underlying the plate. Assuming a model of elastic flexure, the very small wavelengths (5 - 30km) characteristic of Qiangtang basins would then imply extremely thin (1-5 km) effective elastic plate thicknesses. These very low values are difficult to reconcile with any reasonable characterization of crustal rheology. Instead, these relatively small basins likely record the creation of accommodation space created by differential uplift across the strike of folds and faults. Stratal geometries and sedimentation rates reflect the kinematics and geometries of local compressional structures and the mechanical basis for the creation of accommodation space remains uncertain. Finally, the origin of these basins makes it unlikely that early Tertiary sedimentation represents a significant fraction of the upper crust of Tibetan plateau.

T42B-0297 1330h POSTER

Age of Initiation of the India-Asia Collision in the eastern Himalayas

Bin Zhu (518-437-43760; zhub@atmos.albany.edu)

William Kidd[1] (518-442-4466; wkidd@atmos.albany.edu)

David Rowley[2] (rowley@plates.uchicago.edu)

Brian Currie[1,3]

[1]University at Albany, 1400 Washington Avenue, Albany, NY 12222, United States

[2]University of Chicago, 5734 S.Ellis Avenue, Chicago, Il 60637, United States

[3]Miami University, 114 Shideler Hall, Oxford, OH 45056, United States

We report on the provenance of the Jidula and Zongpubei Formations, located in the early Tertiary terrigenous sediments of the Tingri region, southern Tibet, which were deposited on the former northern margin of the Indian continent. Petrographical analysis of sandstones reveals that the monocrystalline quartz grains of cratonic origin are dominant in the Paleocene (Danian) Jidula Formation; in contrast there are significant amounts of immature framework grains with a distinct ophiolitic and volcanic arc influence present in the Eocene (Lutetian) Zongpubei Formation. Bulk sample major, trace and rare earth element concentrations in both sandstones and shales complement the petrographical data indicating that the source of the Jidula Formation primarily consisted of quartzose basement rocks, probably of Indian continental origin, while the Zongpubei Formation samples are mainly derived from an arc-trench system indicating the start of obduction of the Asian arc/subduction complex (Gangdese-Xigaze) during the deposition of the Zongpubei sedimentary rocks. The probe compositions of Cr-rich spinels in the Zongpubei sandstones are closely similar to those from fore-arc peridotites, so are most likely derived from the arc and ophiolite rocks along the Yarlung-Zangbo suture to the north. No spinels have been observed in the Jidula sandstones. These early Tertiary detrital clastics in the Tingri region record a marked change in provenance and sediment character starting with the deposition of the Zongpubei Formation. This change indicates that the onset of India-Asia collision and development of the foreland basin on the Indian passive margin started at 47 Ma in the eastern part of the Himalayas. This is about 4 Ma younger than the age determined by Garzanti et al.(1987, 1996) in the Zanskar section of the western Himalayas.

T42B-0298 1330h POSTER

Mesozoic-Cenozoic history of subduction within the Tethyan region as inferred from seismic tomography and plate tectonic reconstructions

Edith Hafkenscheid[1] (+31 30 2537503; hafkensc@geo.uu.nl)

Rinus Wortel[1]

Wim Spakman[1]

[1]Faculty of Earth Sciences, Utrecht University, P.O. Box 80021, Utrecht 3508 TA, Netherlands

We have studied the large-scale history of subduction within the Tethyan region, the Alpine-Himalayan-Indonesian mountain chain that stretches from the Mediterranean to Southeast Asia. From tomographic images of the present mantle structure, the volumes and locations of the positive seismic velocity anomalies are determined. The large tomographic volumes, and the large depths at which they are found, indicate that they must have resulted from long periods of subduction in Cenozoic and Mesozoic times. We therefore examine the large-scale surface motions within the region since 200 Ma, the time window that is thought to be necessary to explain the inferred tomographic anomalies. From plate tectonic reconstructions, the amount of convergence and velocities, both relative and absolute, are determined using the relevant poles of rotation. In general, we find the tomographic volumes in the upper mantle in the eastern Mediterranean and Middle East to be similar to the tectonic volumes that are expected to have subducted during the Cenozoic. On the contrary, the results indicate that the Cenozoic amount of shortening in the Indian region was probably not accompanied by lithosphere subducting into the mantle. For all regions, the tomographic volumes found in the lower mantle are larger than the tectonic volumes expected to have subducted during mainly Mesozoic times. The volumes in the Indian region and the Middle East approximately differ a factor 1-2. However, the results suggest that much more material must have been subducted in the eastern Mediterranean than is calculated for the African-Eurasian convergence alone. This points to a major role of oceanic spreading during lithospheric subduction in the area.

T42B-0299 1330h POSTER

Variations of Standard Deviation of Gravity Anomalies in Chugoku District, Japan: Relationship with Distributions of Topographic Lineaments

Takeshi Kudo[1] (kudou.takeshi@jnc.go.jp)

Tsuyoshi Nohara[1] (nohara@tono.jnc.go.jp)

Hirohisa Kinoshita[1] (kinoshita.hirohisa@jnc.go.jp)

Akihiko Yamamoto[2] (star@eos.hokudai.ac.jp)

Ryuichi Shichi[3] (shichi@isc.chubu.ac.jp)

[1]Tono Geoscience Center, Japan Nuclear Cycle Development Institute, 1-63, Yamanouchi, Akeyo, Mizunami 509-6132, Japan

[2]Graduate School of Science, Hokkaido University, N10S8, Kita-ku, Sapporo 060-0810, Japan

[3]College of Engineering, Chubu University, Matsumoto-cho, Kasugai 487-8501, Japan

Relationship between distribution of topographic lineaments and variation of standard deviation of gravity anomalies in Chugoku district, Japan is investigated. Tectonic movement may disturb lateral continuities of crustal structures at weak zones. Lateral discontinuities of the density structure cause undulations of gravity anomaly field over them. Therefore, complexities of the gravity anomaly field might be an indicator of the past crustal instability. On the other hand, topographic lineaments are formed along zones of inherent crustal weakness, and the gravity anomaly complexity relates to distribution of surface lineaments. In order to verify this conjecture, we investigated gravity anomaly complexities in relation to the spatial distributions of topographic lineaments.

As an index of complexity of gravity anomaly field, we employed standard deviation (SD) of Bouguer anomalies. We divided the survey area into a set of regular grid cells with a mesh size of 1 km x 1 km, to the centers of which we assigned a representative SD value calculated from Bouguer anomalies inside a given search area. In this study, the nodes are centered in the regular grid cells and we used a circled search area centering at each node. We also need to revise the array data in a point-registered file of topographic lineaments because the distance between two neighboring points along each lineament does not have a constant value. The average distance is 186 m, and the standard deviation is 294 m. These deviations of the distances between neighbor points may cause implausible results. In order to import this lineament data into a statistic analysis, we reproduced a new set of array data with the constant value of 10 m for the distance between them. Then, we made a statistical analysis by referring the Bouguer anomaly SD values to the numbers of the lineament data points within 3 km from each node. Thus, we repeated the present method while the search radii for the SD determination are 5, 10, 15 and 20 km.

Frequency distribution of the lineament data points to SD values showed that locations of the lineaments tend to overlap the high SD areas of gravity anomaly field. These results imply an applicability of SD of Bouguer gravity anomalies in order to discuss the crustal weakness and the instability. Furthermore, this index derived from gravity anomaly might be effective even over the area covered by thick sediments and/or volcanic products, where fault-like structures are hard to be detected.

T42B-0300 1330h POSTER

Active Continental Growth During Transpressional Tectonics: Example from Southeastern Taiwan

Chia-Yu Lu[1] (chia@ntu.edu.tw)

Yu-Chang Chan[2] (yuchang@earth.sinica.edu.tw)

Jian-Cheng Lee[2] (jclee@earth.sinica.edu.tw)

Hao-Tsu Chu[3] (chuht@linx.moeacgs.gov.tw)

Jacques Malavieille[4] (malavie@dstu.univ-montp2.fr)

[1]Department of Geosciences, National Taiwan University, 245, Choushan Road, Taipei 106, Taiwan

[2]Institute of Earth Sciences, Academia Sinica, Taiwan, 128 Academia Road Sec. 2, Nankang, Taipei 115, Taiwan

[3]Central Geological Survey, MOEA, 2. Lane 109, Hua-Hsin Street, Chung-Ho, Taipei 235, Taiwan

[4]Lab. Geophysics, Tectonics, and Sedimentology,, Univ., Montpellier II, 4, PL E Bataillon, Montpellier 34060, France

Based on structural analysis and regional kinematics data from GPS measurements, we propose a tectonic evolution model for the active continental growth in the southeastern Taiwan. The deformation structures in the Miocene deposits of the southeastern Central Range exhibit characteristics of early-stage orogenic processes. These brittle-ductile deformation features indicate complex tectonic processes involved, including underthrusting, exhumation, and left-lateral transpressional movements. The observed deformation processes in the southeastern Central Range evidently combine together and interact within a single, complex framework. In the E-W transects across the Central Range, regional foliation orientations generally display a fan-shaped pattern with dips to the mountain core on both sides. In addition, kilometer-scale overturned structures were mapped at the eastern flank of the southern Central Range, the earlier foreland thrust and fold structures were largely overturned. This overall upward flower structure is consistent with an early-proposed exhumation and vertical accretion model. In general, the kinematics data suggest left-lateral transpressional tectonic movement is currently important process in the southeastern Taiwan. And under such tectonic movement, we highlight the contribution of the Luzon arc accretion to the continental growth of East Asia.

T42B-0301 1330h POSTER

Preliminary Identification of Major Faults in the Namche Barwa: Results from a NASA Shuttle Radar Topography Mission (SRTM) DEM Calibrated With Field Mapping and Seismicity

Amanda L Ault[1] (610.758.3669; ala2@lehigh.edu)

Anne S Meltzer[1] (610.758.3673; ameltzer@lehigh.edu)

William S F Kidd[2] (518.442.4477; wkidd@atmos.albany.edu)

[1]Lehigh University, Department of Earth and Environmental Sciences 31 Williams, Bethlehem, PA 18015, United States

[2]University at Albany, DEAS - ES351, Albany, NY 12222, United States

One of the most striking features of the Himalayan eastern syntaxis, Tibet, is the Tsangpo River Gorge, whose erosive power has created over 7000 m of local relief in the region of Namche Barwa. The erosion rate at Namche Barwa is rapid relative to other parts of the Himalaya, and the geodynamic/surface interaction is hypothesized to be very similar to the tectonic aneurism identified in the western syntaxis (Nanga Parbat and the Indus River, Pakistan) by Zeitler et al. (2001). Although the Namche Barwa is rapidly eroding, most of the active faults that accommodate exhumation have not been mapped. Based on the hypothesis that underlying tectonic processes are recorded in distinct topographic signatures, this study utilizes the NASA seamless Shuttle Radar Topography Mission (SRTM) digital elevation model (DEM) in conjunction with seismicity and field mapping to identify potential locations of active faults in this rapidly-eroding region for further field investigation. This type of calibration of remote-sensed DEM and TM (ETM+) data with field mapping and seismicity can by applied to identify active faults in other regions, such as the politically- and

geographically-restricted southeastern portion of Namche Barwa or other remote sites on Earth, a critical first step in forming topographic descriptions that can determine where and how the landscape is responding to underlying geodynamic processes. Globally, unprecedented opportunities for remote studies of topography will arise as more 90-m SRTM and data of similar resolution are released, and it is timely to further characterize their uses and limits.

URL: http://ees.lehigh.edu

T42B-0302 1330h POSTER

Wavelet-based Fusion Of Panchromatic ETM+ And Multispectral ASTER Images Covering The Neoproterozoic Allaqi-Heiani Suture,Southeastern Egypt

Dianwei Ren[1] (972-883-2447; rencui@utdallas.edu)

Mohamed G Abdelsalam (972-883-2447; abdels@utdallas.edu)

[1]Mohamed G. Abdelsalam, Department of Geosciences, The University of Texas at Dallas Box 830688 Richardson TX 75083-0688, Richardson, TX 75080, United States

The Allaqi-Heiani Suture is a WNW-ESE trending deformation zone defined by a S-verging fold and thrust belt and is dominated by volcano-sedimentary rocks, dismembered ophiolites, and syn- and post-tectonic granitoids. The Advanced Space-borne Thermal Emission and Reflection Radiometer (ASTER) data covering this area is processed by performing the Optimum Index Factor (OIF) analysis for the purpose of selecting the optimum Red-Green-Blue (RGB) color cpombinations. ASTER data have fourteen bands; 3 in Visible and near infrared (VNIR) with 15 m spatial resolution; 6 Short wave infrared (SWIR) with 30 m spatial resolution, and 5 in the Thermal infrared (TIR) with 90 m spatial resolution. Therefore, the selected RGB color combinations from ASTER data are sometimes have poor spatial resolution. The Enhanced Thematic Mapper Plus (ETM+) panchromatic band with 15 m spatial resolution covering the same area is used to enhance the spatial resolution of ASTER images. The ETM+ panchromatic bands and the multispeectral RGB color combinations from ASTER data are fused together to incorporate the higher spatial resolution of the ETM+ panchromatic band (high frequency information) and the better spectral characteristics (low frequency) of the ASTER bands. Two- and multi-band wavelet transformations are performed for three newly generated ETM+ panchromatic bands based on three histograms that corresponds to those of the three ASTER bands used in the fusion. Three approximation, low frequency images and numerous exact, high frequency images are obtained each time from the ETM+ panchromatic bands. The low frequency information in the ASTER bands (better spectral information) and the high frequency information in the ETM+ panchromatic band (better spatial resolution) are fused together. Hence, the 3 approximation (low frequency) images obtained from the two-band wavelet or multi-band wavelet for the ETM+ panchromatic band are replaced by the three selected ASTER bands, respectively. Three new bands are generated by performing the inversed wavelet transformation for the approximation images from ASTER bands and the corresponding detailed bands from the ETM+ band are used to generate new RGB color combination images. The results from the two-band wavelet and multi-band wavelet are compared with each other and also with other fusion techniques such as RGB-Hue-Saturation-Intensity (HSI-RGB and Color Normalization Transformation (CNT). Wavelet-based fusion proved to be advantageous in retaining better spectral characteristics of multi-spectral ASTER data and incorporating the better spatial resolution of the panchromatic ETM+ data. geological features which were not obvious in either images or images produced by RGB-HSI-RGB and CNT fusion techniques were revealed more clearly in images generated by wavelet-based fusion.

T42C MCC: 2002-2004 Thursday 1340h

At the Seismogenic Front: Dynamic Processes at Convergent Margins III

(joint with G, S)

Presiding: **D Saffer,** University of Wyoming; **D Cardace,** Washington University

T42C-01 1340h INVITED

Geodetic and Seismic Constraints on some Seismogenic Zone Processes in Costa Rica

Tim Dixon (tdixon@rsmas.miami.edu)

University of Miami, RSMAS, 4600 Rickenbacker Cswy, Miami, FL 33149, United States

E. Norabuena (UM/RSMAS), S. Schwartz and H. DeShon (UCSC) L. Dorman (SIO), E. Flueh (GEOMAR), P. Lundgren (JPL), A. Newman, F. Pollitz (USGS), M. Protti (OVSICORI). We report results from joint seismic (on-land PASCAL and offshore OBS) and geodetic (GPS) observations in Costa Rica designed to elucidate seismogenic zone processes related to subduction of the Cocos plate beneath the western edge of the Caribbean plate. For the Nicoya peninsula, where our seismic deployment was longer, the seismic data are used to constrain the geometry of the plate interface for purposes of modeling the geodetic data. Seismogenic zone events here show significant updip variability, corresponding to changes in subducted oceanic crust origin and heat flow. Inversion of the GPS data here suggests a patchy distribution of locked zones, with two relatively small, elliptically shaped locked zones elongated parallel to the trench (centered on 14 and 38 km depth) within a larger region of low locking (or possibly freely slipping), as well as northeast motion of a coastal "sliver block" at 8 plus/minus 3 mm/yr associated with oblique convergence. In contrast, for the Osa peninsula, there is no evidence of trench-parallel motion (convergence here is orthogonal) and the entire plate interface to a depth of about 50 km appears to be fully locked. In addition, the southwest-dipping block boundary on the Caribbean coast separating the Panama block and Caribbean plate also appears to be fully locked and accumulating strain, with shortening rates of about 1-2 cm/yr. The large zone of locked slip on the main plate interface beneath the Osa Peninsula, as well as the associated "back-arc" deformation, is presumably related to subduction of the shallow Cocos Ridge and consequent high compressive stress in the direction of plate convergence. Over geologic time, this may promote crustal shortening in the region, and uplift of the Cordillera Talamanca in southern Costa Rica.

T42C-02 1355h

Inter-plate coupling in Nicoya Peninsula, Costa Rica, as deduced from trans-peninsula GPS experiment

Takeshi Iinuma[1] (81-3-5841-5736; iinuma@eri.u-tokyo.ac.jp); Jorge Marino Protti[2] (jprotti@una.ac.cr); Koichiro Obana[3] (obanak@jamstec.go.jp); Victor González[2] (vgonzale@una.ac.cr); Rodolfo Van der Laat[2] (rvanderl@una.ac.cr); Teruyuki Kato[1] (teru@eri.u-tokyo.ac.jp); Shin'ichi Miyazaki[1] (miyagsi@pangea.stanford.edu); Yoshiyuki Kaneda[3] (kaneday@jamstec.go.jp); Enrique Hernandez[2] (ehernan@una.ac.cr)

[1]ERI, Univ. of Tokyo, 1-1-1, Yayoi, Bunkyo-ku, Tokyo 113-0032, Japan

[2]OVSICORI-UNA, Apartado 2346-3000, Heredia , Costa Rica

[3]IFREE, JAMSTEC , 2-15 Natsushima-cho, Yokosuka 237-0061, Japan

We investigate state of plate coupling at the subduction zone beneath Nicoya Peninsula, northwestern Costa Rica, from 1.5-years of trans-peninsula GPS campaign measurement. Inter-plate coupling zone beneath Nicoya Peninsula is recognized as a clear seismic gap named "Nicoya seismic gap". In this area, Cocos plate is subducting beneath the Caribbean plate from the Mid American Trench with large convergence rate about 90mm/yr, and because of this, large earthquakes have occurred in 1853, 1900, and 1950 at this segment, and two large earthquakes occurred around Nicoya peninsula (M_W7.0 in 1990 to the SE and the 1992 M_W7.6 off Nicaragua to the NW). In the Nicoya seismic gap, a strong coupling of the two plates is manifested by low background seismicity, the sharp edge of aftershock zone of the 1990 and 1992 earthquakes, and the northeastward movement of the Nicoya peninsula recorded with GPS observations.
We started a new GPS survey program in Nicoya peninsula in 2001 to obtain new knowledge about the seismic coupling and the potential earthquake. 7 new benchmarks for GPS campaign observation were installed completing a 10-sites transect across Nicoya peninsula. We have done 3 times of GPS campaign observation on this array.
Crustal deformation on inter-seismic period above Nicoya seismic gap is estimated from 1.5 years of GPS observations. Obtained velocity field suggests that the forarc sliver motion along the pacific coast of Nicoya peninsula produces 8.5mm/yr of northwestward motion parallel to the Mid American Trench.
We performed an inversion analysis to infer inter-plate coupling at Nicoya seismic gap. The result of the inversion shows that upper and lower limits of coupling zone are corresponding with ones of seismogenic zone, which was investigated by Newman *et al.* (2002) with seismological methods. Accumulated strain in the Nicoya seismic gap is able to bring earthquake whose moment magnitude is larger than 7.5.

T42C-03 1410h

Aseismic Slip and Stress Transfer in Guerrero, Southern Mexico

Anthony R. Lowry[1] (303-492-5141; arlowry@himalaya.colorado.edu)

Kristine M. Larson[2] (Kristine.Larson@colorado.edu)

Vladimir Kostoglodov[3] (vladi@servidor.unam.mx)

Osvaldo Sanchez[3] (osvaldo@servidor.unam.mx)

Kenneth W. Hudnut[4] (hudnut@gps.caltech.edu)

[1]Department of Physics, University of Colorado, Boulder, CO 80309-0390, United States

[2]Department of Aerospace Engineering Science, University of Colorado, Boulder, CO 80309-0492, United States

[3]Instituto de Geofisica, UNAM, Mexico D.F. 04510, Mexico

[4]U.S. Geological Survey, 525 S. Wilson Ave., Pasadena, CA 91106, United States

Geodetic measurements from Guerrero, southern Mexico, show evidence for at least four large transient slip events in 1995, 1998, 2002 and 2003. Inverse modeling of the data suggests that the steady-state slip on the plate-boundary thrust includes partial frictional coupling at depths greater than 25 km, producing a slip deficit which is partially or completely relieved during aseismic slip events, and strong frictional coupling on the shallow thrust which is not relieved aseismically. Slip events have been observed down-dip of the seismogenic zone at several other subduction zones including New Zealand, Japan, Alaska and Cascadia. In many cases, these are interpreted as repeating events that activate a similar area on the thrust at regular intervals. In Guerrero, however, the behavior is more complex: Quiescent intervals range from one to four years, and moment release in these four events varies by up to an order of magnitude. Spatial distributions also vary substantially between events. Perhaps the most consistent feature of the events is the timescale: Significant anomalous slip lasted about three to four months during all three events observed by continuous GPS. The events are also characterized by widespread activation of slip. The current network of continuous GPS sites covers an area of about 480 km strike-parallel by 270 km strike-perpendicular, but in all events there remains the possibility that slip extended well beyond the instrumental coverage. In this presentation, we will examine the potential role of these slip events as agents for stress transfer, and assess the possibility that they are initiated by stress changes during seismic events of magnitude 6 and higher on or near the thrust.

T42C-04 1425h

Episodic Forearc Uplift Related to Subduction of the Woodlark Basin, Western Solomons Arc: Intermittent Aseismic Slip or Multi-Century Earthquake Recurrence Intervals?

Frederick W Taylor[1] (512-471-0453; fred@ig.utexas.edu); Cliff Frohlich[1] (512-471-0460; cliff@ig.utexas.edu); Paul Mann[1] (paulm@ig.utexas.edu); G. S. Burr[2] (burr@u.arizona.edu); Warren Beck[2] (wbeck@physics.arizona.edu); R. L. Edwards[3] (edwar001@maroon.tc.umn.edu); David A. Phillips[4] (dap@soest.hawaii.edu)

[1]Institute for Geophysics, Univ. Texas, 4412 Spicewood Springs Rd., Austin, TX 78759-8500, United States

1710 h **SM42E-05** Calibrating a Magnetotail Model for Storm/Substorm Forecasting: **W Horton**, S Siebert, M Mithaiwala, I Doxas

1725 h **SM42E-06** *INVITED* Vector and Scalar Field Visualization Techniques for Multispacecraft Space Physics Missions: **D A Roberts**, V Rezapkin, J Coleman, R Boller

1745 h **SM42E-07** Visualization and Data Analysis for CISM Models: **M Wiltberger**, T Guild, J G Lyon

---

T42A MCC: Level 1 Thursday 1330h
The Structure and Physical Properties of Grain Boundaries in Rocks III Posters *(joint with V)*

Presiding: **A Schubnel**, Lassonde Institute; **S Majumder**, University of Minnesota

1330 h **T42A-0265** *POSTER* Mechanical compaction of Bleurswiller sandstone : elastic wave velocities and permeability evolution: **J Fortin**, A Schubnel, Y Gueguen

1330 h **T42A-0266** *POSTER* Reduction of ionic diffusivity in nanopore water of geomaterials: **T Hirono**, S Nakashima, C J Spiers

1330 h **T42A-0267** *POSTER* An Experimental Study of Pressure Solution of Halite Under the Confocal Microscope: **Z Karcz**, E Aharonov, D M Ertas, R J Johnston, R S Polizzotti, C H Scholz

1330 h **T42A-0268** *POSTER* Mobility of Water Molecules on Brucite and Talc Surfaces by *Ab Initio* Potential Energy Surface and Molecular Dynamics Simulations: **H Sakuma**, T Tsuchiya, K Kawamura, K Otsuki

1330 h **T42A-0269** *POSTER* The Influence of Second Phases on Grain Boundaries of Mylonitic Microfabrics: Evidences From Natural Carbonate Mylonites: A Ebert, **M Herwegh**, A Pfiffner

1330 h **T42A-0270** *POSTER* A Close View Into the 3D Geometry of Grain-to-Grain Contacts and Surface Roughness in Sandstones Using Laser Scanning Confocal Microscopy: B Menendez, C David, **L Louis**, A Martinez Nistal

1330 h **T42A-0271** *POSTER* On Grain Boundary Wetting During Deformation: **S Majumder**, P H Leo, D L Kohlstedt

1330 h **T42A-0272** *POSTER* Connectivity of molten Fe alloy in mantle peridotite based on in situ electrical conductivity measurements: **T Yoshino**, M J Walter, T Katsura

1330 h **T42A-0273** *POSTER* Compositional effect on the dihedral angle between olivine and Fe-S liquid up to 20 GPa: Possibility of percolative core formation: **H Terasaki**, D C Rubie, D J Frost, F Langenhorst

1330 h **T42A-0274** *POSTER* The role of interfaces in plastic flow of two-phase rocks: X Xiao, G Dresen, **B Evans**

1330 h **T42A-0275** *POSTER* Melt-Grown Grain Textures of Eutectic Mixtures of Water Ice with Magnesium- and Sodium-Sulfate Hydrates and Sulfuric-Acid Hydrate Using Cryogenic SEM (CSEM): **C McCarthy**, S Kirby, W Durham, L Stern

1330 h **T42A-0276** *POSTER* Investigation Of The Transition To Nonlinear Acoustics In Driven Rods: **D Pasqualini**, T Jim, S Habib, K Heitmann, P Johnson

1330 h **T42A-0277** *POSTER* α-β Inversion in Quartz From Low Frequency Electrical Impedance Spectroscopy: **N Bagdassarov**

1330 h **T42A-0278** *POSTER* Damage and elastic recovery of calcite-rich rocks deformed in the cataclastic regime: **A Schubnel**, J Fortin, L Burlini, Y Gueguen

1330 h **T42A-0279** *POSTER* Modeling constitutive behavior and compaction localization for high porosity sandstone: **E R Grueschow**, J W Rudnicki

1330 h **T42A-0280** *POSTER* Rheological Behaviour and Microstructures of Natural Gypsum Experimentally Deformed in Simple Shear: **V Barberini**, L Burlini, E H Rutter, M Dapiaggi

1330 h **T42A-0281** *POSTER* Physical Properties of the Interface between a Mineral Inclusion and the Host Mineral: Monazite Inclusions in Fluorapatite: **D E Harlov**, R Wirth, H Foerster

1330 h **T42A-0282** *POSTER* The Impact of Olivine-Orthopyroxene Phase Boundaries on Mechanical Absorption: Inferences from Resonant Ultrasound Spectroscopy (RUS): J Lan, Y Wang, R S Lakes, **R F Cooper**

1330 h **T42A-0283** *POSTER* Anomalous Thermal Relaxation Induced by the Granular Composition of Berea Sandstone: **T Ulrich**, K R McCall, R Guyer

1330 h **T42A-0284** *POSTER* Microstructural Evolution and Grain Boundary Structure During Static Recrystallization in Synthetic Polycrystals of Sodium Chloride Containing Saturated Brine: J Urai, **O Schenk**

1330 h **T42A-0285** *POSTER* Grain-Scale Distribution of Aqueous Fluid in Wherlites: **T Ouchi**, M Nakamura

---

T42B MCC: Level 1 Thursday 1330h
The Tectonics of Tibet and East Asia Posters

Presiding: **A Meltzer**, Lehigh University; **A L Ault**, Lehigh University

1330 h **T42B-0286** *POSTER* Tectonic Evolution of South China Coastal Provinces Since the Mid-Mesozoic: **L Chan**, M F Pubellier, P V Phung, M Mechti, K F Leung, F Ego

1330 h **T42B-0287** *POSTER* A Lower Paleozoic Plate Tectonic Model for the North Qilian Mountains, NW China: **H Yang**, C Tseng, G Zuo, H Wu, Z Xu, J Yang

1330 h **T42B-0288** *POSTER* Geochemical and Geochronologic Constraints on the Tectonic Evolution of Southeastern Tibet: **A L Booth**, P K Zeitler, W S Kidd, J L Wooden, B Idleman, L Yuping, C P Chamberlain

1330 h **T42B-0289** *POSTER* Tectonic Evolution of Mirs Bay Basin in Guangdong, South China: **K Leung**, L S Chan, M Pubellier

1330 h **T42B-0290** *POSTER* Rising the Himalayan-Tibetan plateau: A 3-D finite element model: **Y Yang**, M Liu

1330 h **T42B-0291** *POSTER* Rapid Erosion at the Tsangpo Knickpoint and Exhumation of Southeastern Tibet: **M A Malloy**, P K Zeitler, B D Idleman, P W Reiners, L Zheng

1330 h **T42B-0292** *POSTER* The Eastern Syntaxis Seismic Experiment: **A Meltzer**, S Sol, B Zurek, Z Xuanyang, Z Jianlong, T Wenqing

1330 h **T42B-0293** *POSTER* Preliminary results of 10Be analyses from the eastern Himalayan syntaxis: evidence for unsteady erosion on two spatial scales.: **N J Finnegan**, B Hallet, J O Stone, D R Montgomery

1330 h **T42B-0294** *POSTER* Kinematic modeling of Neotectonic velocity field of the Persia-Tibet-Burma Orogen: **Z Liu**, P Bird

1330 h **T42B-0295** *POSTER* Source Mechanisms, Velocity Structures and Himalaya Tectonics: **F T Wu**, A F Sheehan, G Huang, G Monsalve

1330 h **T42B-0296** *POSTER* Mechanisms for creating accommodation space during early Tertiary sedimentation in Tibet.: **C Studnicki-Gizbert**, B C Burchfiel

1330 h **T42B-0297** *POSTER* Age of Initiation of the India-Asia Collision in the eastern Himalayas: **B Zhu**, W Kidd, D Rowley, B Currie

1330 h **T42B-0298** *POSTER* Mesozoic-Cenozoic history of subduction within the Tethyan region as inferred from seismic tomography and plate tectonic reconstructions: **E Hafkenscheid**, R Wortel, W Spakman

1330 h **T42B-0299** *POSTER* Variations of Standard Deviation of Gravity Anomalies in Chugoku District, Japan: Relationship with Distributions of Topographic Lineaments: **T Kudo**, T Nohara, H Kinoshita, A Yamamoto, R Shichi

1330 h **T42B-0300** *POSTER* Active Continental Growth During Transpressional Tectonics -V Example from Southeastern Taiwan: **C Lu**, Y Chan, J Lee, H Chu, J Malavieille

1330 h **T42B-0301** *POSTER* Preliminary Identification of Major Faults in the Namche Barwa: Results from a NASA Shuttle Radar Topography Mission (SRTM) DEM Calibrated With Field Mapping and Seismicity: **A L Ault**, A S Meltzer, W S Kidd

1330 h **T42B-0302** *POSTER* Wavelet-based Fusion Of Panchromatic ETM+ And Multispectral ASTER Images Covering The Neoproterozoic Allaqi-Heiani Suture,Southeastern Egypt: **D Ren**, M G Abdelsalam

---

T42C MCC: 2002-2004 Thursday 1340h
At the Seismogenic Front: Dynamic Processes at Convergent Margins III *(joint with G, S)*

Presiding: **D Saffer**, University of Wyoming; **D Cardace**, Washington University

1340 h **T42C-01** *INVITED* Geodetic and Seismic Constraints on some Seismogenic Zone Processes in Costa Rica: **T Dixon**

1355 h **T42C-02** Inter-plate coupling in Nicoya Peninsula, Costa Rica, as deduced from trans-peninsula GPS experiment: **T Iinuma**, J M Protti, K Obana, V González, R Van der Laat, T Kato, S Miyazaki, Y Kaneda, E Hernandez

1410 h **T42C-03** Aseismic Slip and Stress Transfer in Guerrero, Southern Mexico: **A R Lowry**, K M Larson, V Kostoglodov, O Sanchez, K W Hudnut

1425 h **T42C-04** Episodic Forearc Uplift Related to Subduction of the Woodlark Basin, Western Solomons Arc: Intermittent Aseismic Slip or Multi-Century Earthquake Recurrence Intervals?: **F W Taylor**, C Frohlich, P Mann, G S Burr, W Beck, R L Edwards, D A Phillips

1440 h **T42C-05** *INVITED* Earthquake Recurrence along the Kuril Trench: A New View from Paleoseismology: **K Satake**, F Nanayama

1455 h **T42C-06** Heat flow distribution and thermal regime across the Nankai accretionary complex: **M Kinoshita**, S Goto, H Hamamoto, M Yamano

1510 h **T42C-07** 3-D Numerical Modeling of Rupture Sequences of Large Shallow Subduction Earthquakes: **Y Liu**, J R Rice

1525 h **T42C-08** Stress interaction between subduction earthquakes and forearc strike-slip faults: Modeling and observations: **U S Ten Brink**, J Lin

---

T42D MCC: 3007 Thursday 1340h
Deformation Mechanisms: From the Lab to the Lithosphere II *(joint with V, MR)*

Presiding: **D L Goldsby**, Brown University

1340 h **T42D-01** Viscosity of a molten mantle: experimental data for liquid peridotite.: **D B Dingwell**, P Courtial, D Giordano, A Nichols

1355 h **T42D-02** Effects of Temperature and Water on Deformation Microstructures of Olivine: **I Katayama**, Z Jiang, S Karato

1410 h **T42D-03** Dislocation Microstructures in Deformed Olivine Displaying the C-type and B-type Fabrics: **T G Sharp**, H Jung, J Fitz Gerald, S Karato

1425 h **T42D-04** Effect of Mineral Reaction on the Deformation of Plagioclase-Olivine Aggregates: **A de Ronde**, H Stünitz, J Tullis

1440 h **T42D-05** DEFORMATION OF SERPENTINITE AND ITS IMPLICATIONS FOR THE ASEISMICITY AND SEISMIC LOW VELOCITY ANOMALY IN SUBDUCTION ZONES: **H Jung**, H W Green

1455 h **T42D-06** HIGH TEMPERATURE DEFORMATION OF OMPHACITE IN ECLOGITE: IMPLICATIONS FOR SUBDUCTED LITHOSPHERE: **J Zhang**, H W Green IIH Jung

1510 h **T42D-07** Nanoindentation Creep of Quartz, Olivine, and Calcite, with Implications for Rate and State Friction Laws: **D L Goldsby**, A Rar, G M Pharr, T E Tullis

1525 h **T42D-08** Nature and Origin of Cataclastic Bands in Well Cemented Quartz Arenite: **J R Farver**, C M Onasch

---

T42E MCC: 2002-2004 Thursday 1700h
Birch Lecture

Presiding: **P Segall**, Stanford University

1700 h INTRODUCTION: P Segall, Stanford

1710 h **T42E-01** *INVITED* Splitting, Stretching and Spreading of Lithosphere: **W Buck**

V42A MCC: Level 1 Thursday 1330h
Frontiers in High-Pressure Research Posters II *(joint with GP, MR, DI)*

Presiding: **L F Dobrzhinetskaya**, Institute of Geophysics and Planetary Physics, University of California, Los Angeles; **J Hu**, Carnegie Institution of Washington

1330 h **V42A-0317** *POSTER* OLIVINE LAMELLAE AND INTERSTITIAL BLEBS OF DIOPSIDE AND ENSTATITE EXSOLVED FROM MAJORITIC GARNET DURING DECOMPRESSION IN MULTIANVIL APPARATUS: **L F Dobrzhinetskaya**, H W Green

1330 h **V42A-0318** *POSTER* Partitioning of H_2O on high pressure phase transformation of olivine: **T Inoue**, T Wada, R Sasaki, T Irifune, H Yurimoto

1330 h **V42A-0319** *POSTER* A Model for Shear Mechanism in the Pyroxene-Ilmenite Transition in $MgSiO_3$: **N Tomioka**

1330 h **V42A-0320** *POSTER* Seismic Properties of Rocks at High PT Conditions. Laboratory Measurements on Mafic and Ultramafic Rocks Representative of Subduction Zones: **R M Prelicz**, L Burlini, K Kunze, J Burg

1330 h **V42A-0321** *POSTER* Diamondiferous Peridotite Tomography: Precursor to Xenolith Dissections.: **L A Taylor**, D S Taylor, M Anand, R Ketcham, W Carlson, N V Sobolev, N Pokhilenko

1330 h **V42A-0322** *POSTER* X-ray Stress Analysis in Deforming Materials: Models and Observations: **L Li**, D J Weidner, W Durham, J Chen, S Mei, M Davis

1330 h **V42A-0323** *POSTER* Torsion Experiments on Wadsleyite under Transition Zone Conditions: **Y Xu**, Y Nishihara, Z Jiang, S Karato

1330 h **V42A-0324** *POSTER* Elasticity of Unquenchable High-Pressure Clinopyroxene at High Pressures and Temperatures: **J Kung**, B Li, T Uchida, Y Wang

1330 h **V42A-0325** *POSTER* The Partial Molar Volume and Thermal Expansivity of Fe2O3 in Alkali Silicate Liquids: Evidence for the Average Coordination of Fe3+: **Q Liu**, R Lange

Eos, Transactions, American Geophysical Union AGU 2003 Fall Meeting Vol. 84, No. 46, 18 November 2003

AGU 2003 Fall Meeting

8-12 December 2003
San Francisco, California

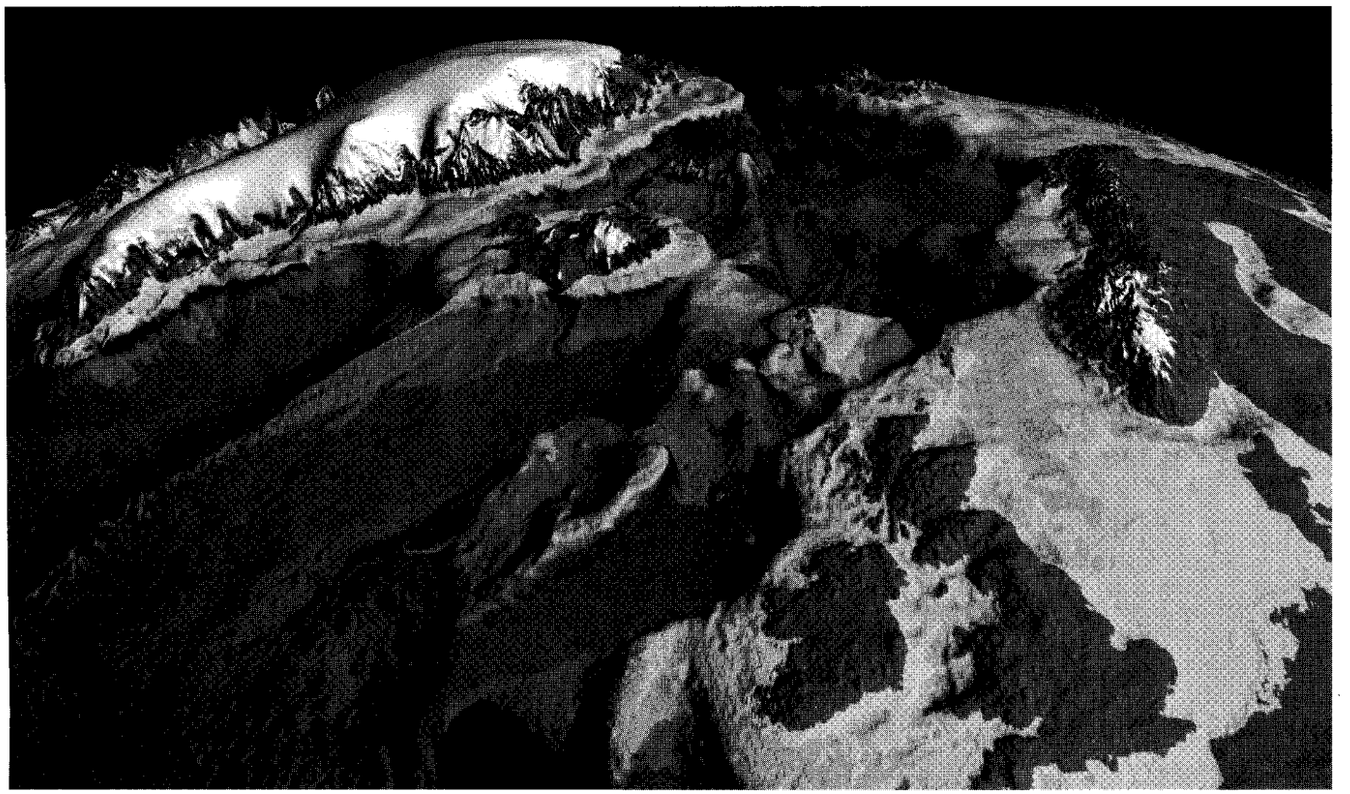

Published as a supplement to
Eos, Transactions, American Geophysical Union
Vol. 84, No. 46, 18 November 2003

AGU